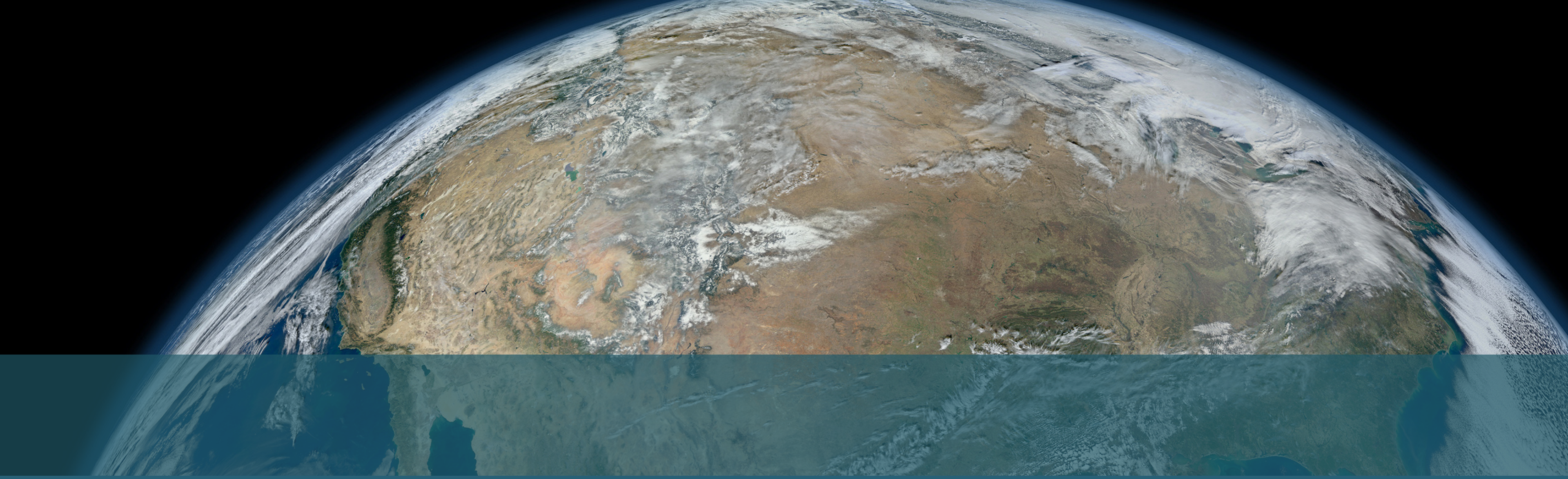

# Relationship Between GOES-R Series Operational Anomalies, In-situ Electron Measurements and Solar Wind Drivers

J. V. Rodriguez[1,2], B. T. Kress[1,2], N. Y. Buzulukova (PI)[3], R. J. Redmon[1],
J. L. Machol[1,2], M. A. Roza[4], J. L. Fiorello[4], R. M. Meloy[5]

[1] NOAA-NCEI CO, [2] CIRES at CU Boulder, [3] NASA-GSFC and Univ. of Maryland, Department of Astronomy,
[4] GSFC GOES-R Program, [5] Science Systems and Applications, Inc.

Spacecraft Anomalies and Failures (SCAF) Workshop 2024
March 27, 2024

*This work was supported by NASA Living With a Star grants 80NSSC19K0085 and NNG19OB09A.*

*Support was also provided by the GOES-R program and the National Centers for Environmental Information (NCEI) through NOAA Cooperative Agreements NA15OAR4320137 and NA17OAR4320101.*

# Outline

- Introduction
- GOES Magnetospheric Particle Sensors (MPS-LO and -HI) Instrument Overview
- Spacecraft Charging and GOES-R Series Spacecraft Operational Anomalies
- Analysis
  - Comparisons between full flux distributions and distributions of fluxes preceding anomalies
  - Superposed Epoch Analysis of GOES-16 electron fluxes
  - Local-time (LT) Dependence of Anomalies and LT-sector-averaged fluxes
  - Association of anomaly occurrence with solar wind high-speed streams
  - Organization of anomalies by inter-anomaly period
- Summary/Conclusions

*Part of this work is from a paper by B. Kress et al. in press in IEEE Transactions on Plasma Science (2024), 'Relationship Between GOES-R Series Spacecraft Operational Anomalies and In-situ 30 eV - 3 MeV Electron Measurements'.*

# The Space Environment In-Situ Suite (SEISS) Magnetospheric Particle Sensors (MPS-LO and -HI)

**Magnetospheric Particle Sensor - Low (MPS-LO)**

- Electrostatic analyzers
- 30 eV-30 keV ions and electrons
- 15 energy channels
- 14 angular zones (12 unique)

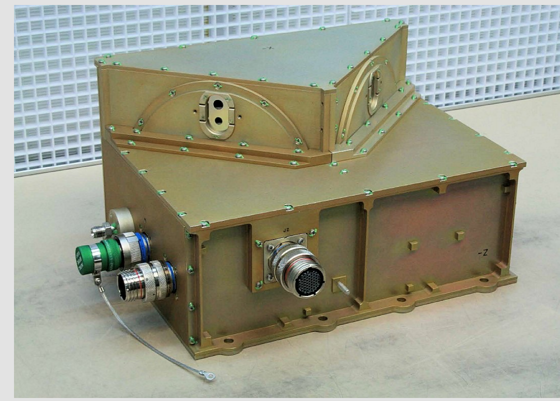

**Magnetospheric Particle Sensor - High (MPS-HI)**

- 5 ion and 5 electron solid state telescopes
- 50 keV-4 MeV electrons in 11 differential channels, plus >2 MeV integral channel
- 80 keV-10 MeV protons in 11 energy bands
- Two hemispherical dosimeters:
  - 100 mil Al: >1.2 MeV electrons, >22 MeV protons
  - 200 mil Al: >2.8 MeV electrons, >37 MeV protons

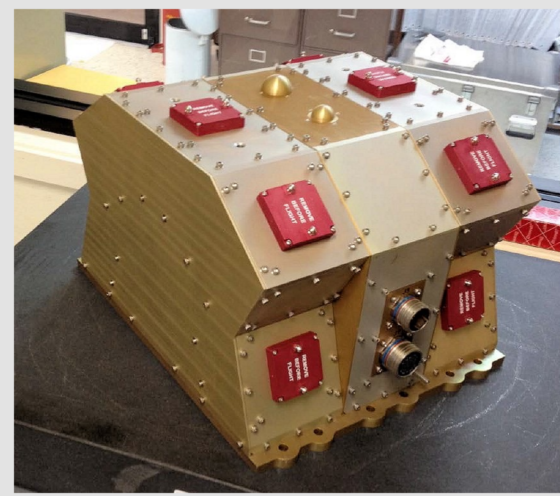

**GOES-16 SEISS began collecting data on 08 Jan. 2017**
**GOES-17 SEISS began collecting data on 24 April 2018**

# Spacecraft Charging

## Spacecraft charging is typically subdivided into two categories:

- Surface Charging
  - Associated with enhancements in 5-10s of keV electron fluxes which can produce elevated potentials on spacecraft surfaces on a timescale of seconds to minutes.
  - May be differential (individual components) or spacecraft frame charging, diagnosed w/ ion line in eV-keV ion data.
- Internal Charging
  - Attributed to 0.1 – 1 MeV electrons which penetrate into dielectric materials causing charge buildup.
  - Timescales for buildup of internal charge is thought to be much longer than surface charging, ranging from hours to >days.
- *The generally accepted electron energy range where there is a transition from surface to internal charging is ~50-100 keV (NASA Handbook 4002A)*

References: NASA Handbook 4002A [2011]; Rodgers & Ryden [2001]; Thomsen et al. [2013].

# EXIS Space Wire (EXS_SPW) Anomaly

- GOES-16 and -17 Operational Anomalies
  - Since launch, a catalogue of recurring GOES-R series operational anomalies has been maintained by the GOES-R program.
  - 1000s of events logged, many involving the spacecraft interface with the solar pointing platform.
- Extreme Ultraviolet and X-ray Irradiance Sensors (EXIS) Space Wire (EXS_SPW) Anomaly
  - All command and telemetry between Solar Pointing Platform (SPP) instruments (x-ray sensor and solar imager) and the spacecraft is handled via the Space Wire interface.
  - This study focuses on one type of anomaly involving telemetry between the Extreme Ultraviolet and X-ray Irradiance Sensors (EXIS) and the spacecraft (EXS_SPW).
  - The EXS_SPW errors are chosen for two reasons:
    - A total of approximately **1750** EXS_SPW events have been cataloged from GOES-16 and -17 combined through 2021, providing good statistics.
    - The EXS_SPW errors exhibit a clear association with periods of elevated energetic electron fluxes.
  - This study uses lists of GOES-16 and -17 EXIS space wire transaction errors cataloged from start of mission (2017 or 2018) through 2021.  The study period spans solar minimum.

# Example of EXS_SPW anomaly 'cluster' w/ 30 eV - 3 MeV electron fluxes

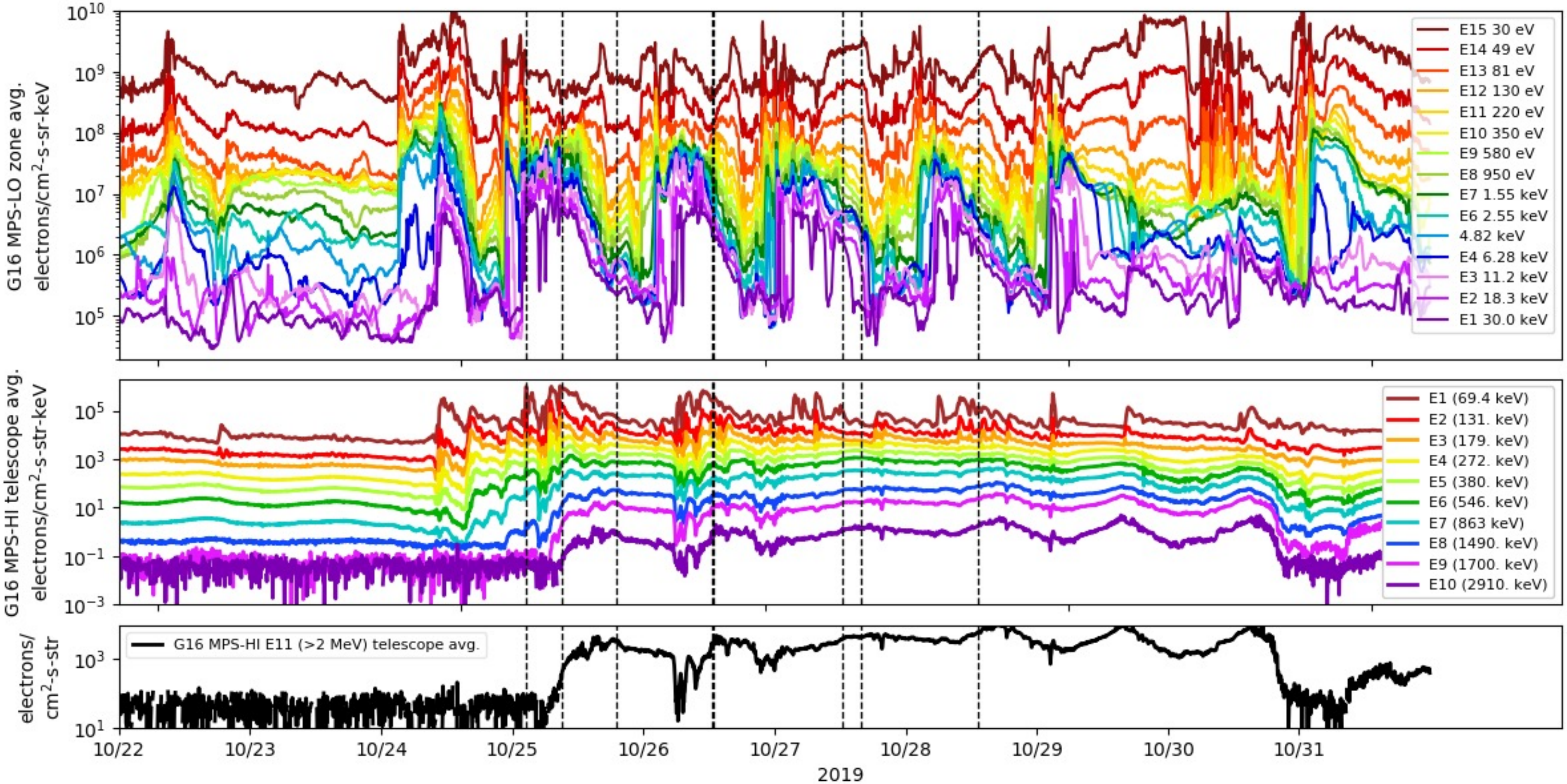

# 2017-2021 MPS-LO and -HI Full and EXS_SPW Anomaly Distributions of 30-min. Avg. Fluxes

**Thick blue dashed**: Full dist. median

**Thin blue dashed**: 25th and 75th percentiles of full dist.

**Red dashed**: Anomaly dist. median

Anomaly dist. median is at full dist. 85th percentile.

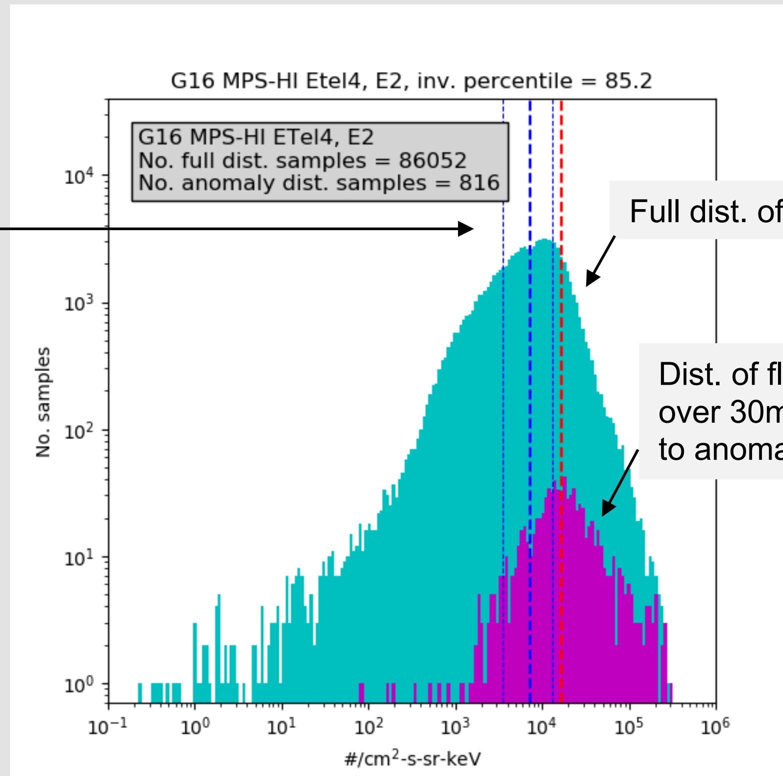


Full dist. of 30-min. avg. fluxes

Dist. of fluxes averaged over 30m interval prior to anomaly

*Full distribution*: Distribution of fluxes averaged over regular 30 min. intervals since MPS-LO and -HI began collecting data in 2017.

*Anomaly distribution*: Distribution of fluxes averaged over 30 min. interval preceding the EXIS Space Wire (EXS_SPW) anomaly.

# Analysis

- Goal is to characterize the difference between the full and anomaly distributions for each energy channel – look direction pair.
- We use 3 tests:
  1. Full distribution percentile at anomaly distribution median
     - Involves use of an inverse percentile function to find the full distribution percentile at the anomaly distribution median flux.
  2. Kolmogorov-Smirnov (two-sample) test statistic
     - Using scipy.stats.ks_2samp
     - Test statistic is max. difference between CDFs of 2 distributions
     - Wikipedia: "What is the probability that these two sets of samples were drawn from the same (but unknown) probability distribution?"
  3. Chi-square test statistic
     - Using scipy.stats.chi2_contingency
- 2 & 3 are well-established tests for statistical dependence/independence.
- No formal formal justification for #1, but it is intuitively appealing and yields approximately the same results as chi-square and K-S tests.
- In each case, the test statistic is taken as a measure of the difference between full and anomaly distributions, rather than used to accept or reject a null hypothesis based on some threshold probability value (standard use).

# GOES-16 2017-2021 Full vs. EXS_SPW Anomaly Distributions of 30-min Avg. Electron Fluxes

*Higher values of test statistic are a measure of greater difference between full and anomaly distributions and more elevated anomaly distribution fluxes with respect to full distribution.*

MPS-LO:
14 look dirs. w/ energy channels

E15: 30 eV
E14: 49 eV
E13: 81 eV
E12: 130 eV
E11: 220 eV
E10: 350 eV
E9: 580 eV
E8: 950 eV
E7: 1,550 eV
E6: 2,550 eV
E5: 4,820 eV
E4: 6,280 eV
E3: 11,200 eV
E2: 18,300 eV
E1: 30,000 eV

MPS-HI:
5 electron telescopes w/ channels

E1: 72 keV
E2: 131 keV
E3: 181 keV
E4: 275 keV
E5: 379 keV
E6: 546 keV
E7: 863 keV
E8: 1.49 MeV
E9: 1.97 MeV
E10: 2.90 MeV
E11: >2 MeV

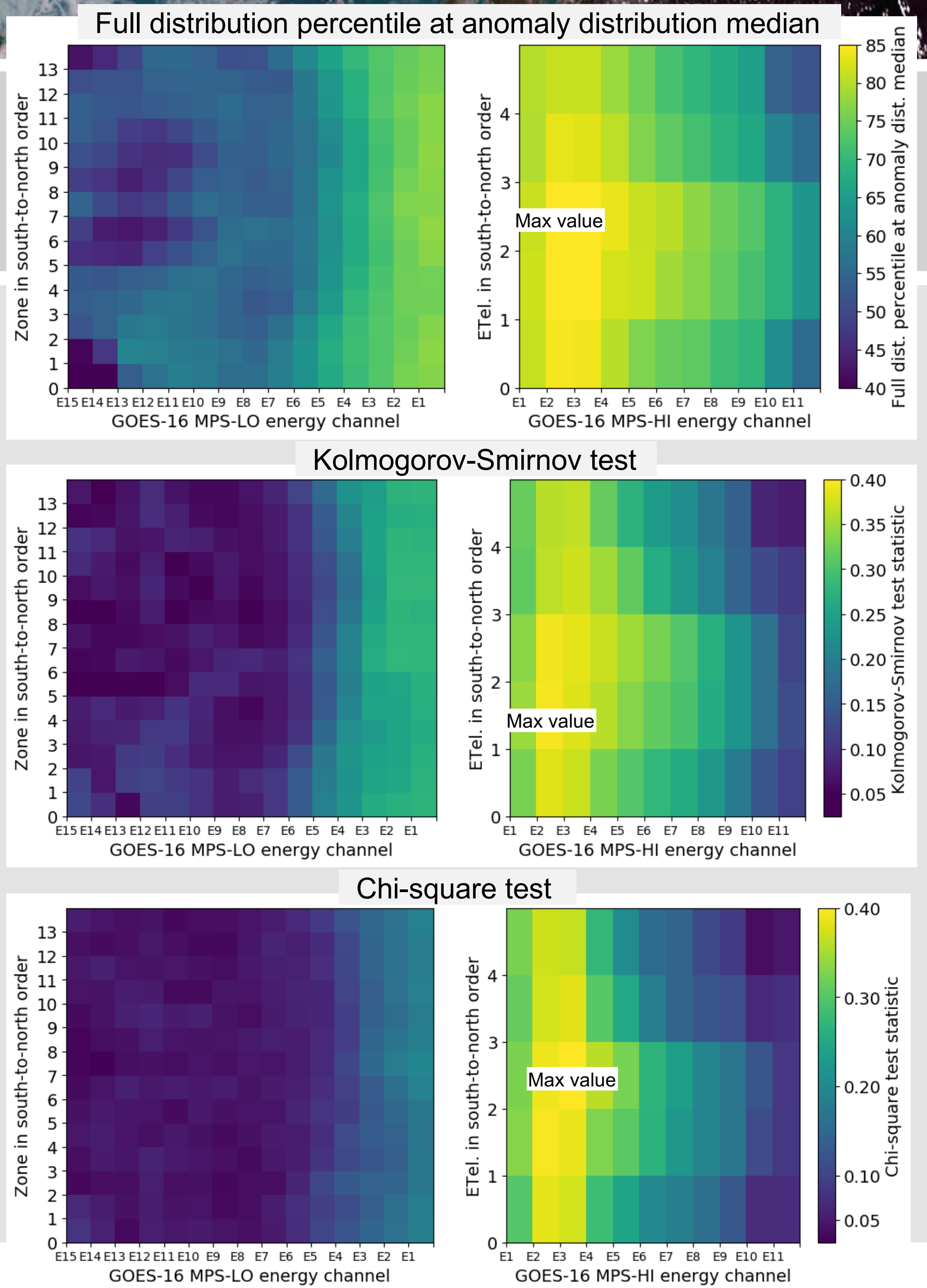

# GOES-17 2018-2021 Full vs. EXS_SPW Anomaly Distributions of 30-min Avg. Electron Fluxes

*Higher values of test statistic are a measure of greater difference between full and anomaly distributions and more elevated anomaly distribution fluxes with respect to full distribution.*

MPS-LO:
14 look dirs. w/ Energy Channels

E15: 30 eV
E14: 49 eV
E13: 81 eV
E12: 130 eV
E11: 220 eV
E10: 350 eV
E9: 580 eV
E8: 950 eV
E7: 1,550 eV
E6: 2,550 eV
E5: 4,820 eV
E4: 6,280 eV
E3: 11,200 eV
E2: 18,300 eV
E1: 30,000 eV

MPS-HI:
5 Electron telescopes w/ channels

E1: 72 keV
E2: 131 keV
E3: 181 keV
E4: 275 keV
E5: 379 keV
E6: 546 keV
E7: 863 keV
E8: 1.49 MeV
E9: 1.97 MeV
E10: 2.90 MeV
E11: >2 MeV

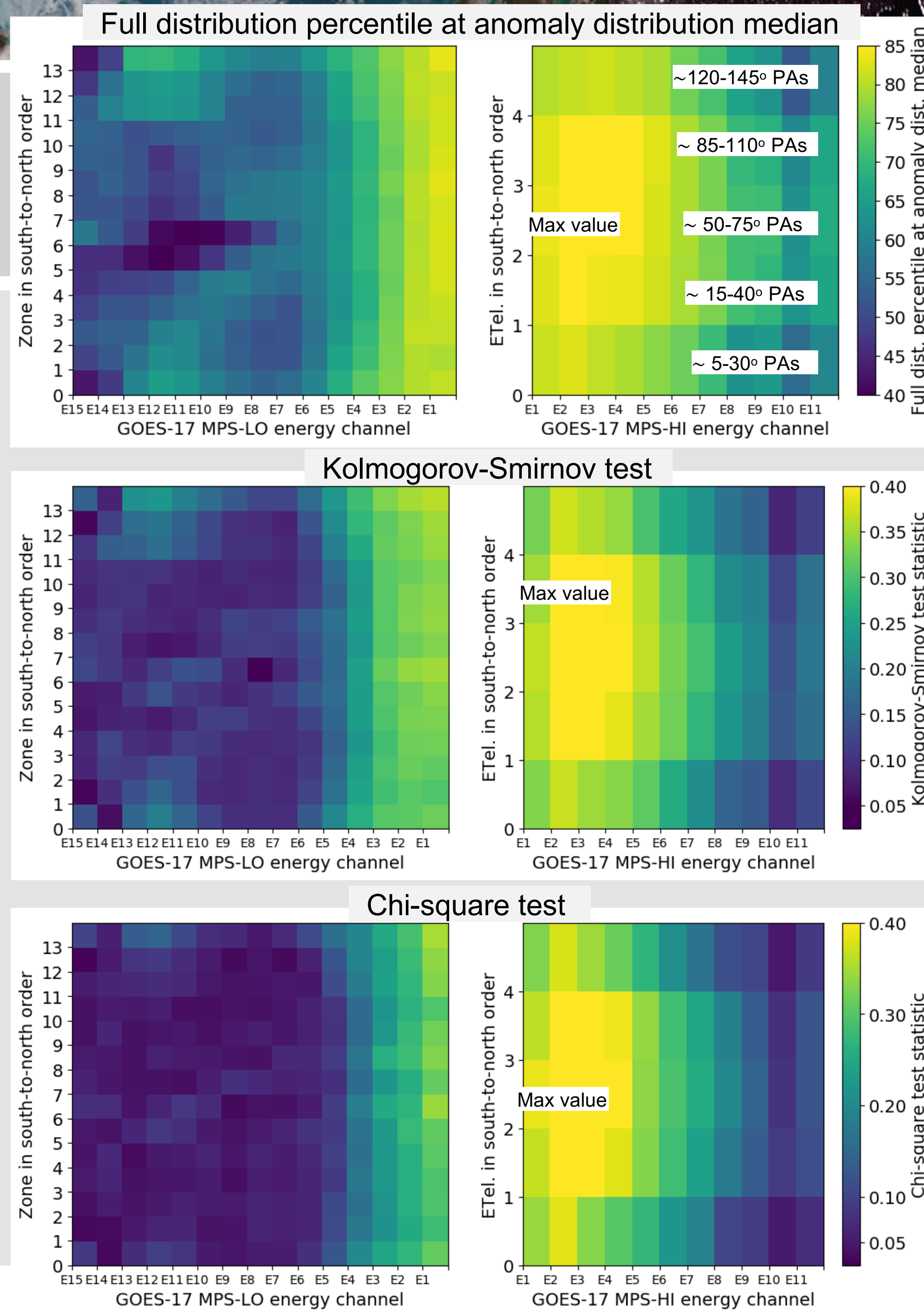

# Local-time (LT) Dependence of EXS_SPW Anomalies and LT sector averaged MPS-HI fluxes

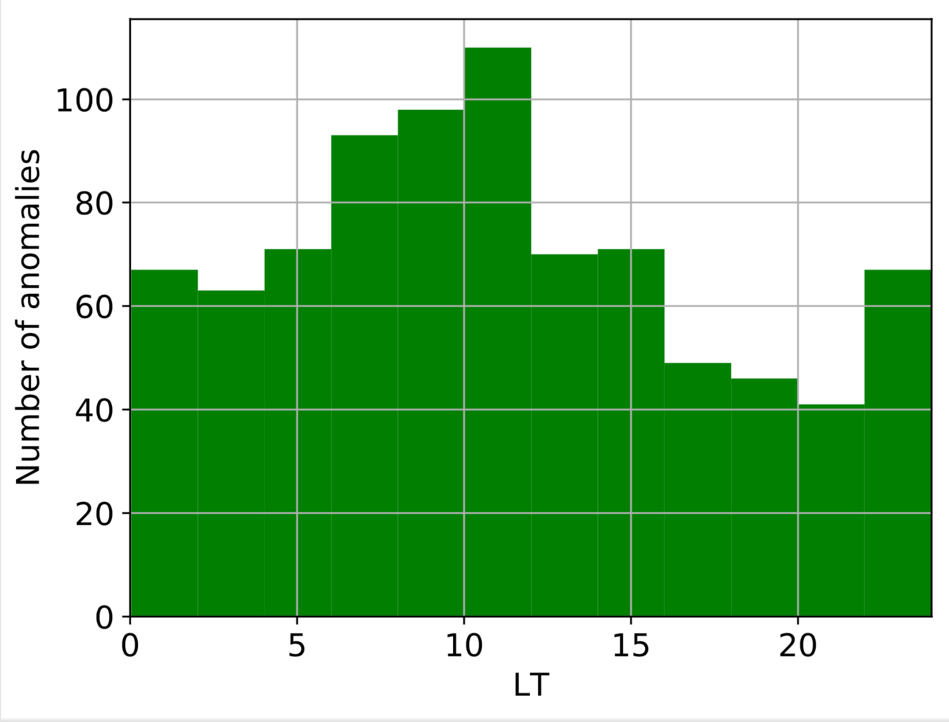


LT dependence of anomalies, showing 846 GOES-16 EXS_SPW anomalies sorted into 2-hour local time bins.

*The delay between the peak in electron flux and anomaly occurrences suggests a charging timescale of ~30 min to several hours, or an LT dependence of conditions more favorable for ESDs.*

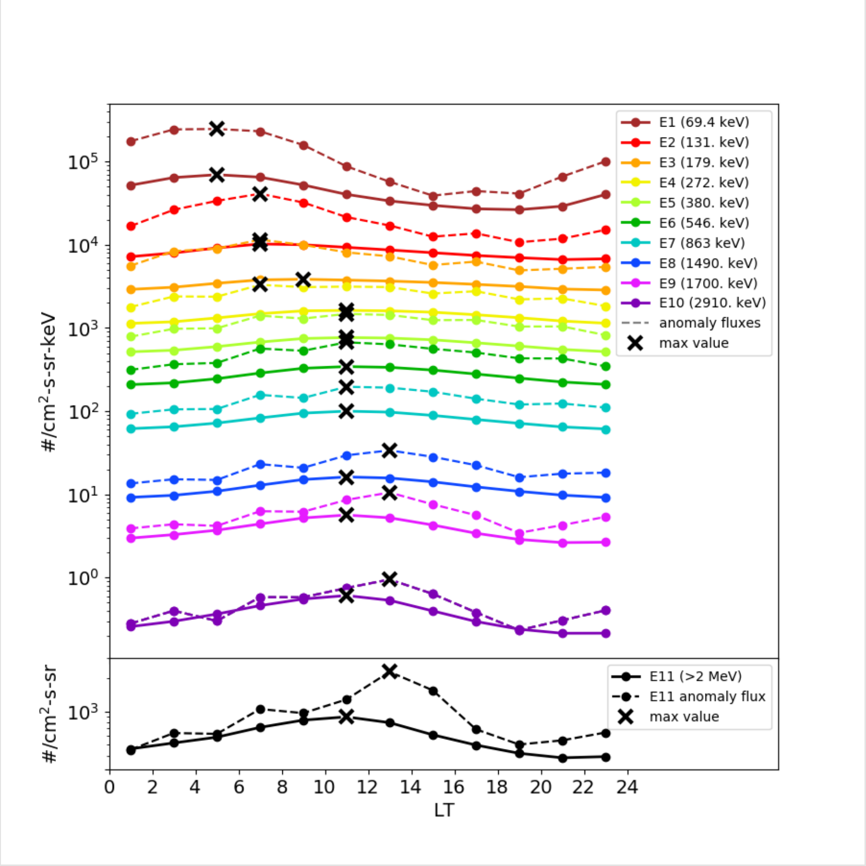


Average GOES-16 MPS-HI fluxes vs. LT, from full (solid) and anomaly (dashed) distributions. 5-minute averaged fluxes are sorted into 2-hour local time bins, then LT sector averages are computed in each bin.
An x-symbol indicates the maximum value along each trace.

# Superposed Epoch Analysis (SEA) of GOES-16 Electron Fluxes

SEA of GOES-16 MPS-LO and -HI zone/telescope averaged fluxes, performed using EXS_SPW events as SEA key time

- Average of 846 5-minute cadence flux time series, each spanning an interval from 12 hours preceding to 12 hours following each anomaly event.
- Each channel normalized using the mean flux from the full flux distribution of all 5-minute flux samples.
- Organizes electron injection peaks in the low 100s of keV into a single peak preceding the anomaly key time.
- Recall: these anomalies occur at all local times.

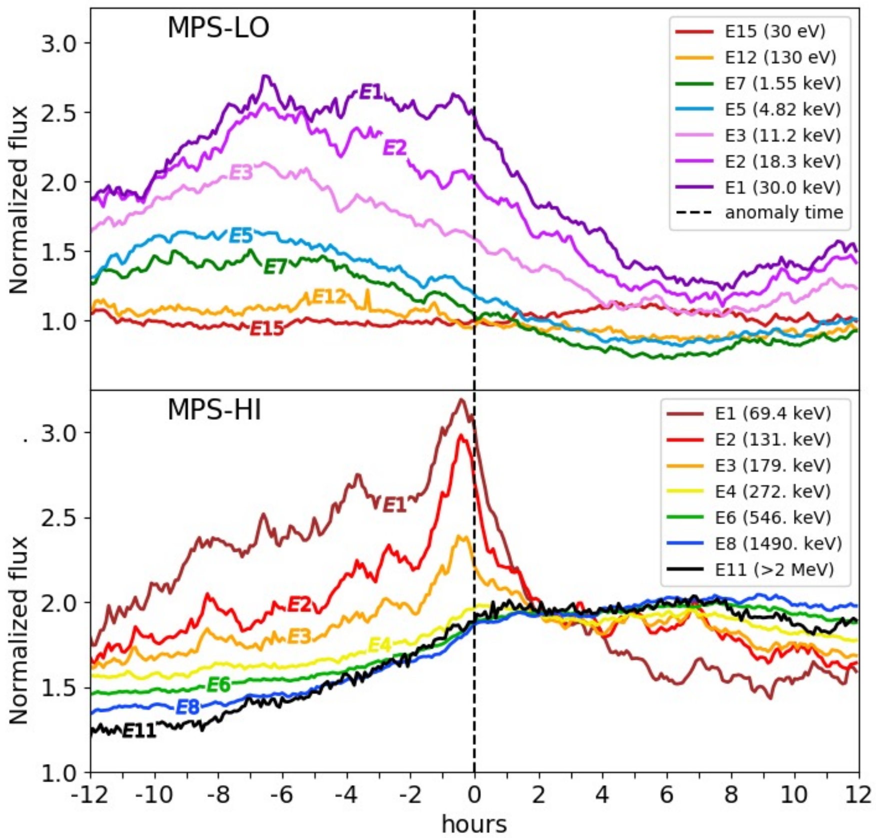

# Anomalies are 'clustered' in relation to high-speed streams and radiation belt enhancements

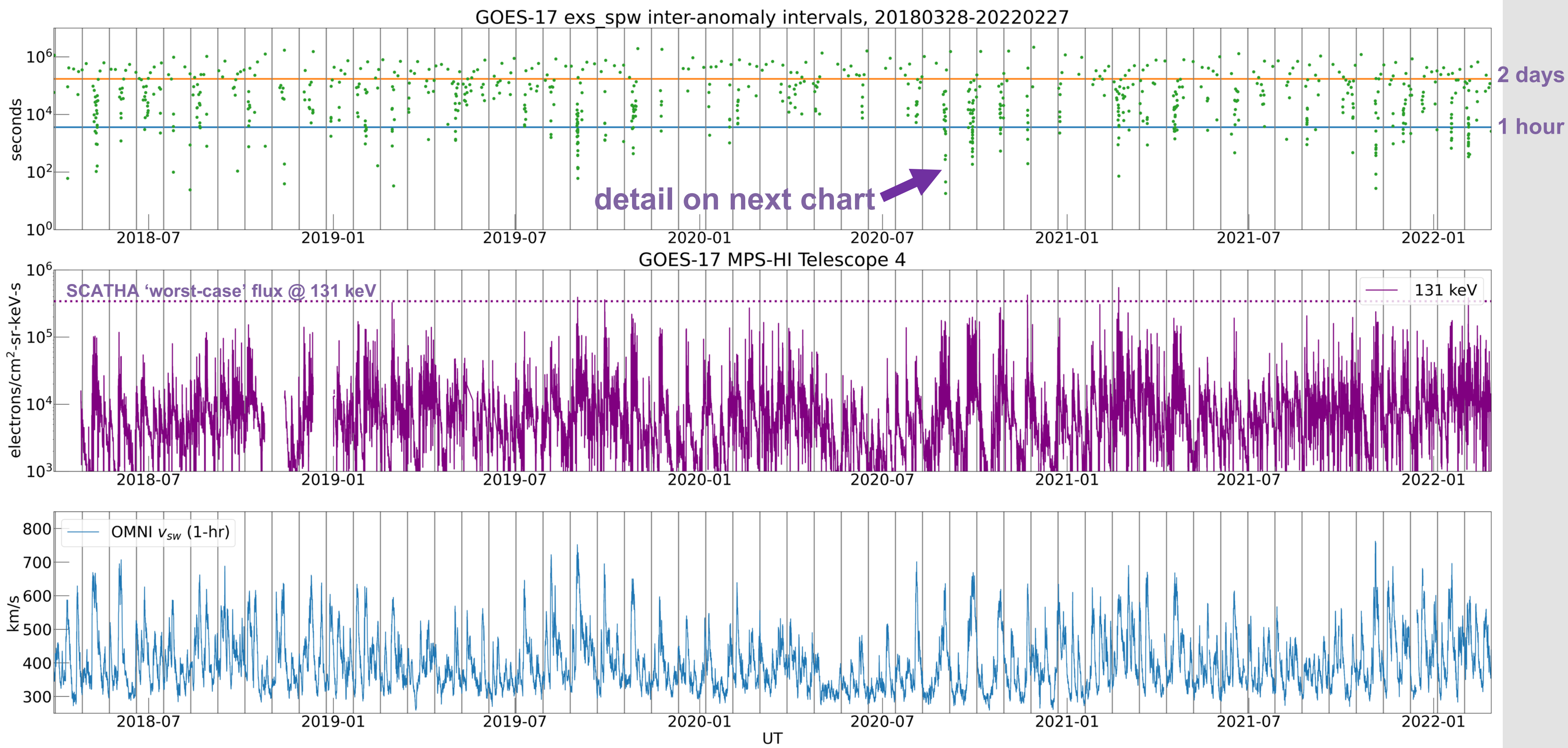

# Anomaly ‘cluster’ example: GOES-16 and -17, 25 August - 8 Sept 2020

***exs_spw inter-anomaly periods, GOES-16***

***0.07-3 MeV electrons, GOES-16***

***exs_spw inter-anomaly periods, GOES-17***

***0.07-3 MeV electrons, GOES-17***

***solar wind speed (Wind)***

***IMF, total and Bz GSM (Wind)***


**2 days**

**1 hour**

**2 days**

**1 hour**

NATIONAL CENTERS FOR ENVIRONMENTAL INFORMATION

# Anomalies per 27-day Solar Rotation Period

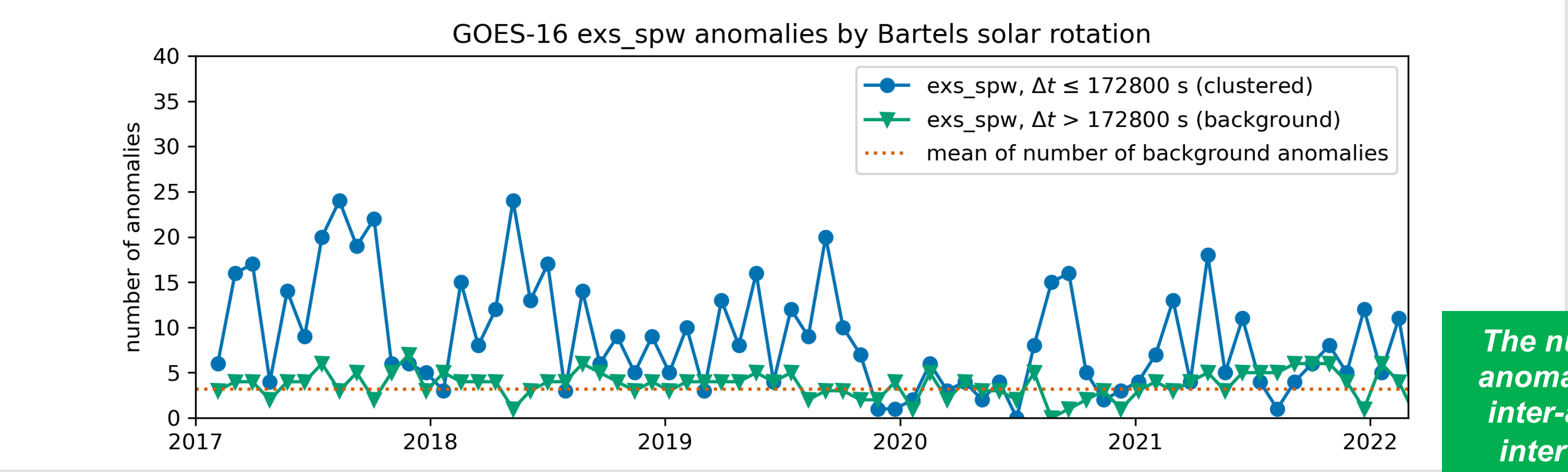


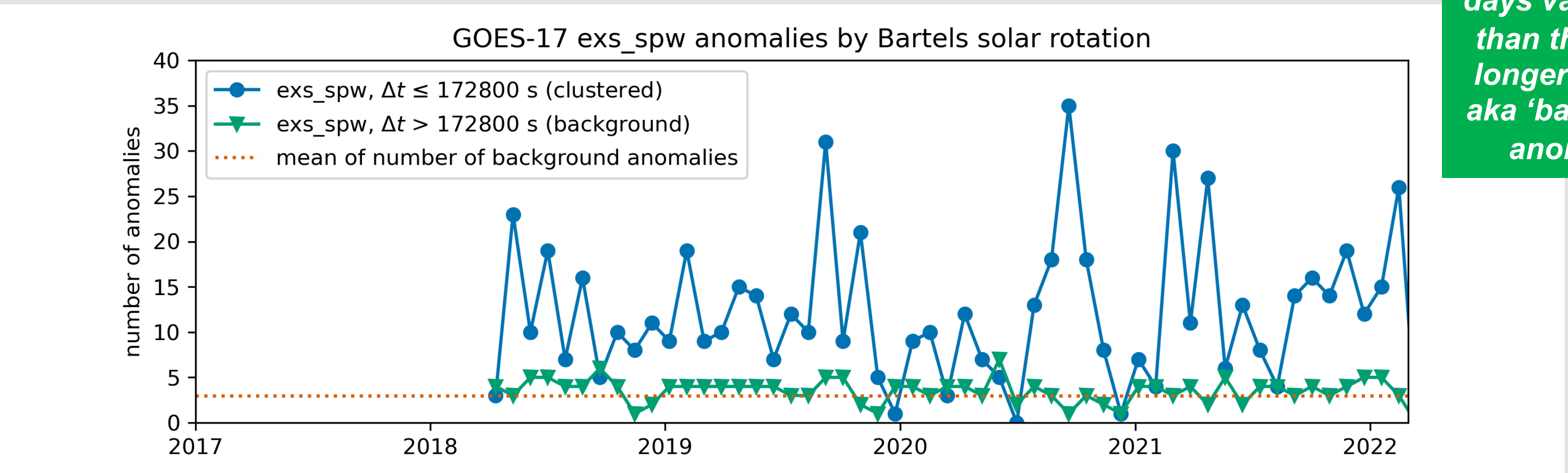


***The number of anomalies with inter-anomaly intervals < 2 days varies more than those with longer intervals aka 'background anomalies'***

# Anomaly LT Distribution: all vs. clustered vs. background

***‘Background’ anomaly distributions are statistically more uniform in local time***

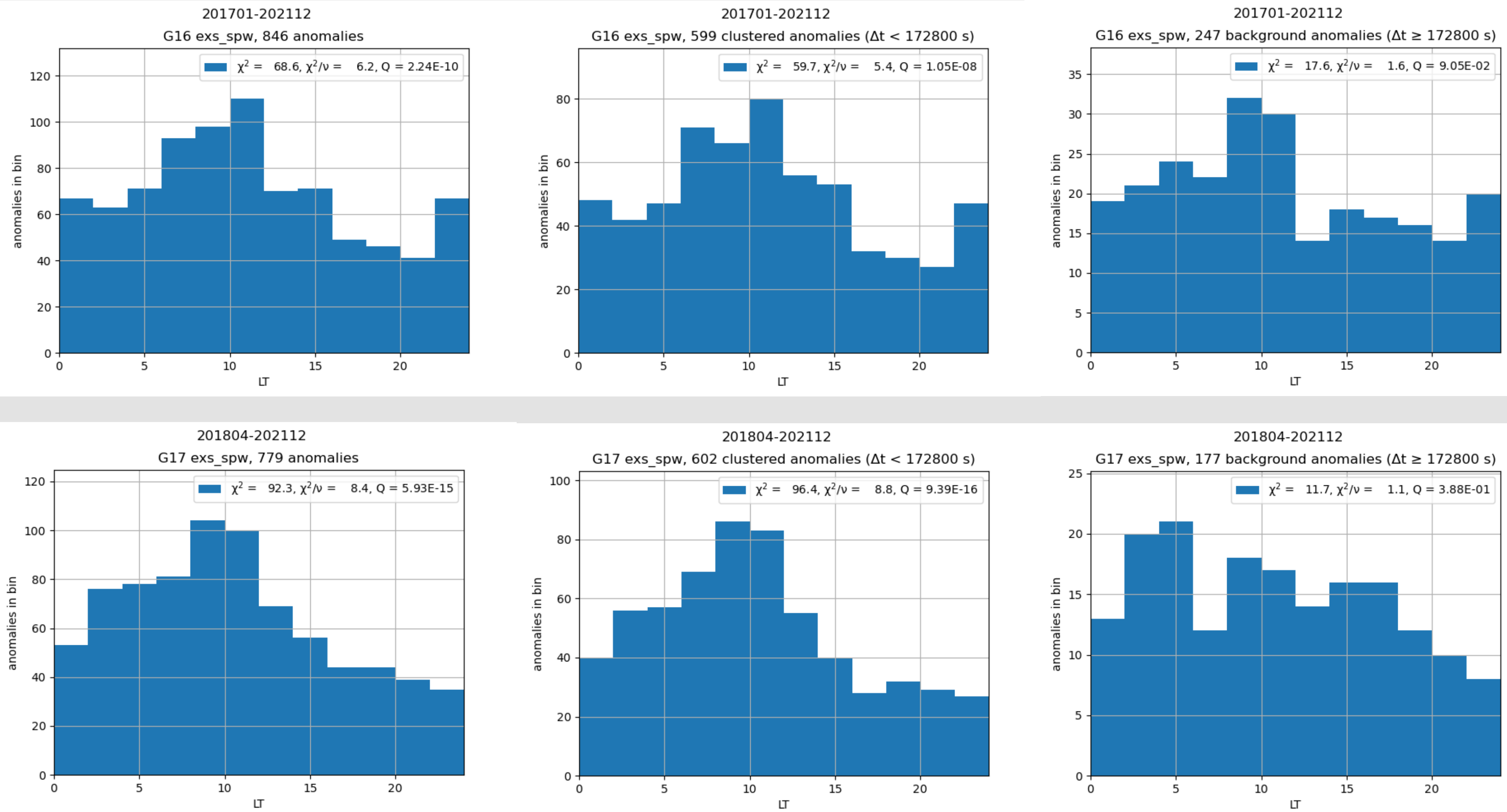

# Anomaly Occurrence during High Speed Streams Originating in Coronal Holes (CH-HSS), 2017-2019

- Use Maris Muntean et al. catalog of CH-HSS during SC24 (2009-2019) (https://www.geodin.ro/varsiti/),
  - HSS = solar wind flow having a jump in speed of >100 km/s from one day to the next and lasting for at least two days
  - Considers only HSS originating in coronal holes (CH) - 117 during this period
- Only 12 ICMEs occurred during 2017-2019 that did not overlap with CH-HSS
  - During solar minimum - does not allow for good statistics on ICMEs
  - Based on Richardson & Cane catalog of ICMEs (1996-2024) (DOI 10.7910/DVN/C2MHTH)
- Basic statistics:
  - What fraction of anomalies occurs during CH-HSS?
  - During which fraction of CH-HSS do anomalies occur?
  - How do the statistics differ between ‘clustered’ and ‘background’ anomalies?

# Statistics of HSS and exs_spw Occurrence

| spacecraft | GOES-16 | GOES-17 |
|---|---|---|
| Number of HSS during MPS-HI observations through 2019 | 117 | 67 |
| Number of anomalies through 2019 | 617 | 374 |
| Fraction HSS with clustered anomalies | 0.62 | 0.61 |
| Fraction HSS with background anomalies | 0.75 | 0.72 |
| Fraction clustered anomalies during HSS | 0.85 | 0.92 |
| Fraction background anomalies during HSS | 0.69 | 0.67 |
| Fraction total duration during HSS | 0.54 | 0.54 |
| Median HSS peak velocity, with anomalies | 590 | 550 |
| Median HSS peak velocity, w/o anomalies | 475 | 472 |

- exs_spw anomalies are more likely to occur during HSS.
- HSS associated with anomalies tend to have greater peak velocities.
- Clustered anomalies are more likely than background anomalies to occur during HSS.

# Bartels Solar Rotation 2511: HSSs Are More Effective Than ICMEs In Driving Anomalies

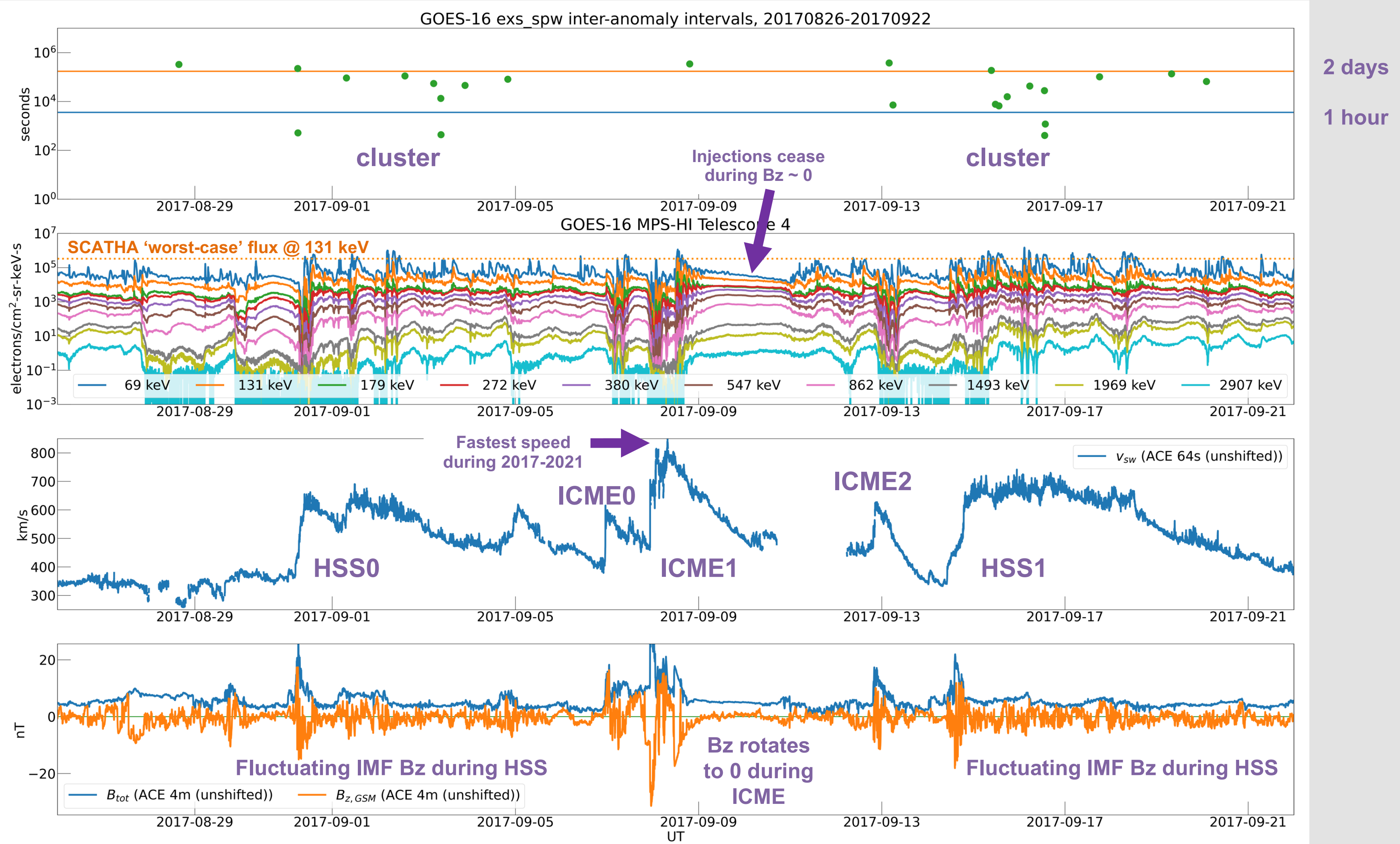

# Summary/Conclusions

- Comparisons of full distributions of measured fluxes and distributions of fluxes preceding the EXS-SPW anomalies show that the anomaly occurrences are most well associated with the elevation of ~130 keV electrons above normal levels, implicating shallow internal charging by electrons in the low 100s of keV.
- This is confirmed by results from superposed epoch analysis showing strong peaks in MPS-HI energy channels in the low 100s of keV preceding the anomalies by ~30 minutes.
- There is a local-time delay between the maximum in LT-sector-averaged ~130 keV electron flux and peak anomaly occurrence rate, suggesting a charging/discharging timescale of ~30 minutes to several hours.
- The dominant solar wind drivers of these anomalies are high-speed streams from coronal holes - the long duration and fluctuating IMF lead to multiple particle injections.
- The anomalies associated with the elevation of ~130 keV electrons occur in clusters with inter-anomaly periods of ~1 minute to 2 days.
- A background of anomalies with > 2 day inter-anomaly periods is more uniform in local time and varies less over multiple solar rotation periods, suggesting another charging location with a longer time constant.

# BACKUP SLIDES

# MLT and Kp Dependence of Anomalies from Surface Charging

*Example:* GOES-4 and -5 experienced 'phantom commands' attributed to ESD from differential surface charging. Based on GOES-4 experience, grounding was added to an instrument radiator on GOES-5 at the launch site.  This fix eliminated only a subset of the 'phantom commands.'

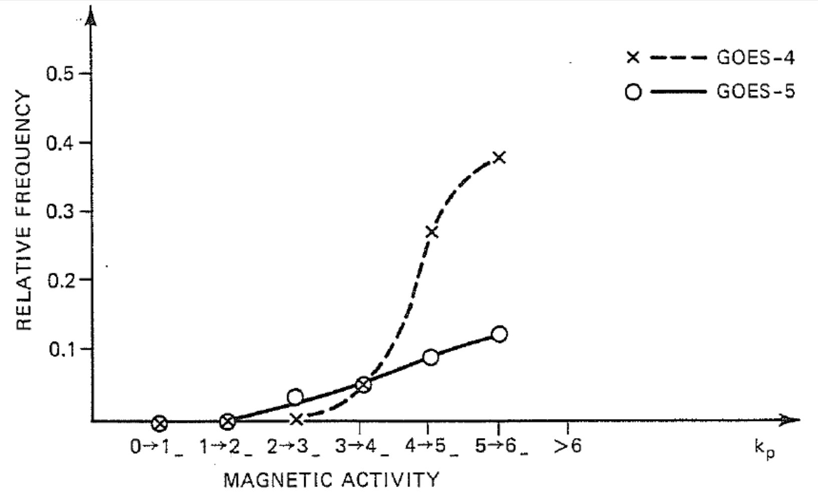


Figure 24. Relative Frequency of Anomalies

Farthing+ 1981, NASA TM 83908

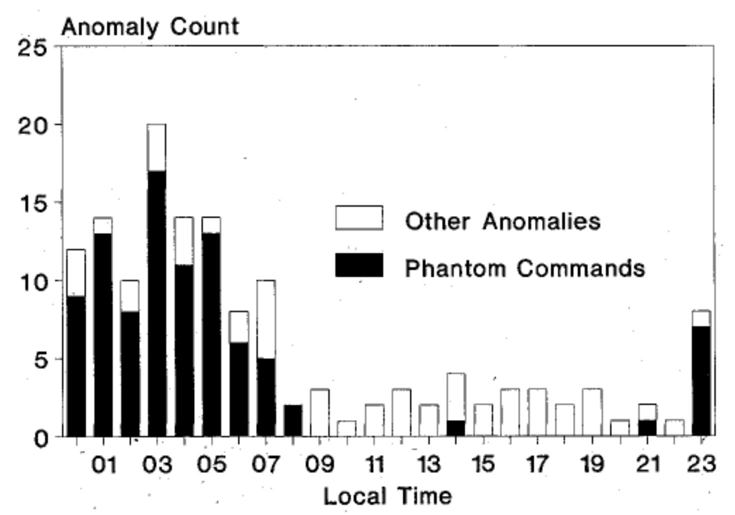


Fig. 2 Local-time distribution of GOES anomalies.

Wilkinson 1994, JSR v. 31, 160-165

# MLT Dependence of Anomalies from Internal Charging

The Distribution of ESD Pulses Observed on SCATHA and Attributed to Internal Discharges was Peaked Near Noon.

Koons+ 2000, Fennell+ 2001

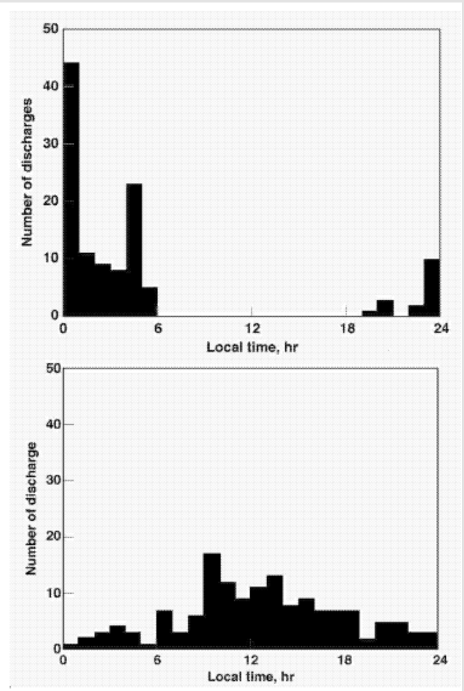


**Figure 5.** Local time distribution of surface discharges in the top panel and internal discharges in the bottom panel.

Inmarsat SSPA Anomalies Observed Between Noon and Dusk Were Attributed to Internal Charging.

Rate of Anomaly Occurrence Increased with Elevated 14- and 21-day >2 MeV Electron Fluence.

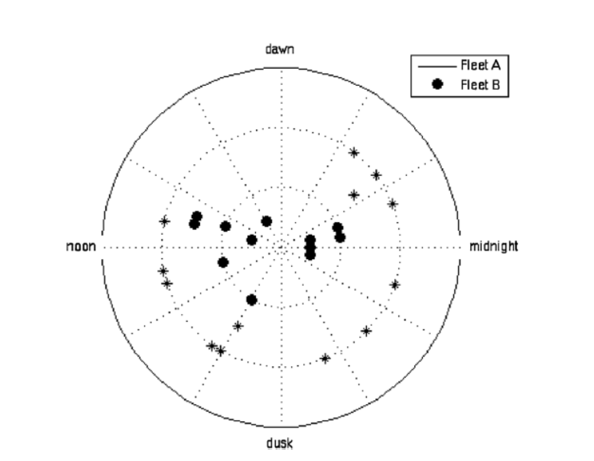


**Figure 7.** Local time for the 26 SSPA anomalies onboard (red circles) Fleet A and (black asterisk) Fleet B. The radial distance from the center of the plot is an offset for clarity and has no other significance.

Lohmeyer & Cahoy 2013; Lohmeyer+ 2015

Dependence of internal charging on geomagnetic activity is reduced by persistence of elevated electron fluxes after storms and by long dielectric time constants.

# exs_spw occurrence increases with Kp up to 6-

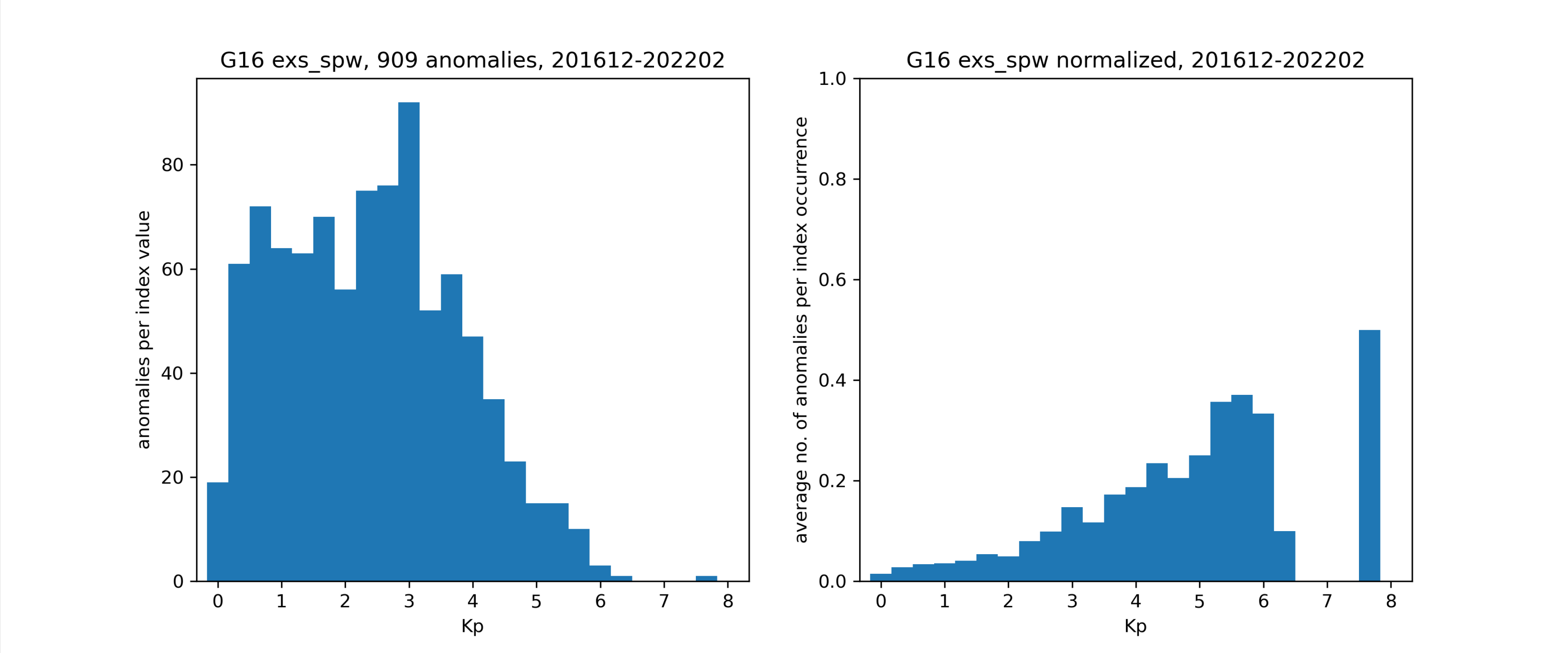


- By comparison, the SEAES-GEO surface charging hazard quotient peaks at Kp = 4 to 5- and is a little lower at Kp = 5 to 6- (O'Brien 2009).

# Additional Results: Consider fluxes averaged over different intervals (in full dist. and prior to anomaly)

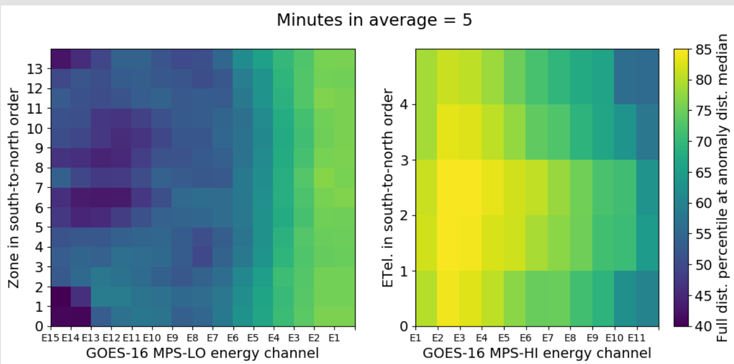


5 min.

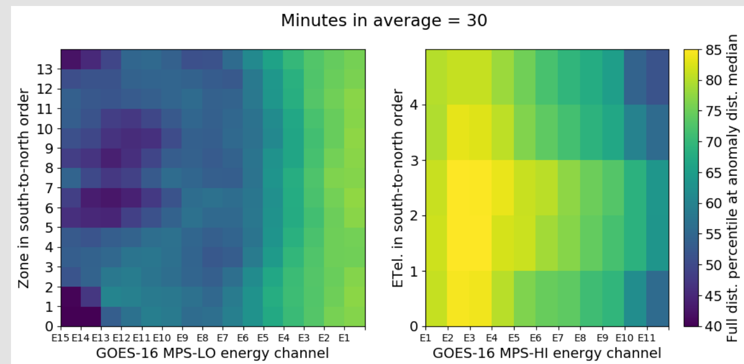


30 min.

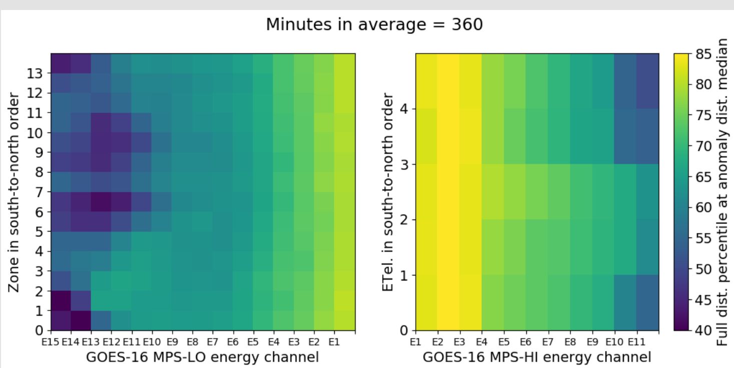


6 hours

Max. value

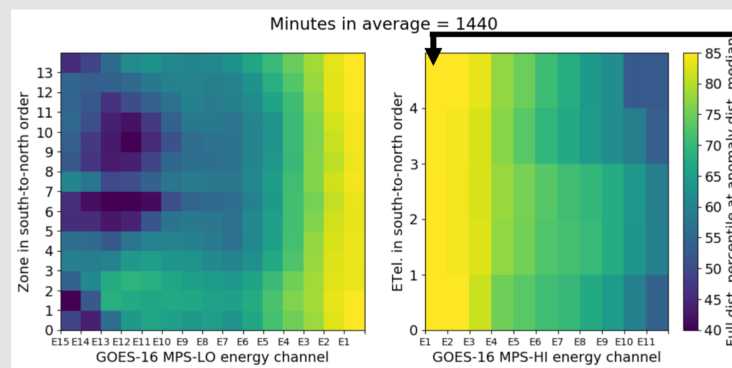


24 hours

Maxima at MPS-HI E2 are persistent for different averaging intervals up to ~24h.

# SCATHA Worst-Case Surface Charging Spectra

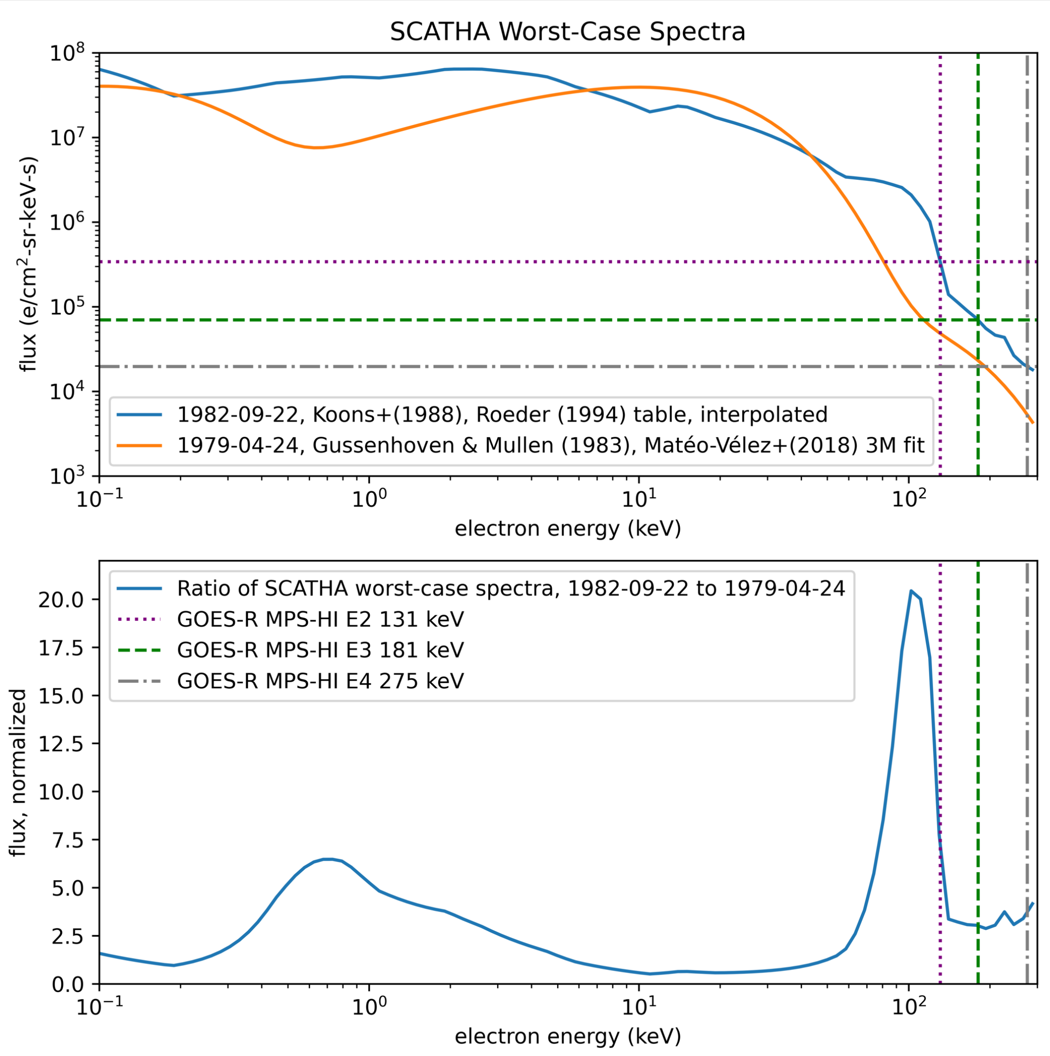

# References


Besliu-Ionescu, D., Maris Muntean, G. & Dobrica, V (2022). Complex Catalogue of High Speed Streams Associated with Geomagnetic Storms During Solar Cycle 24. Sol Phys 297, 65. https://doi.org/10.1007/s11207-022-01998-3

Farthing, W. H., Brown, J. P., & Bryant, W. C. (1981). Differential spacecraft charging on the Geostationary Operational Environmental Satellites. NASA Technical Memorandum 83908.

Fennell, J. F., Koons, H. C., Roeder, J. L., & Blake, J. B. (2001). Spacecraft charging: Observations and relationship to satellite anomalies. Aerospace Report No. TR-2001(8570)-5

Gussenhoven, M. S., & Mullen, E. G. (1983). Geosynchronous environment for severe spacecraft charging. Journal of Spacecraft and Rockets, 20(1), 26-34.

Koons, H. C., Mizera, P. F., Roeder, J. L., & Fennell, J. F. (1988). Several spacecraft-charging event on SCATHA in September 1982. Journal of Spacecraft and Rockets, 25(3), 239-243.

Koons, H. C., Fennell, J. F., & Hall, D. F. (2000). A summary of the engineering results from the Aerospace Corporation experiments on the SCATHA spacecraft. 6th Spacecraft Charging Technology Conference, AFRL-VS-TR-20001578

Lohmeyer, W. Q., and Cahoy, K. (2013), Space weather radiation effects on geostationary satellite solid-state power amplifiers, Space Weather, 11, 476– 488, doi:10.1002/swe.20071.

Lohmeyer, W., A. Carlton, F. Wong, M. Bodeau, A. Kennedy, and K. Cahoy (2015), Response of geostationary communications satellite solid-state power amplifiers to high-energy electron fluence, Space Weather, 13, 298–315, doi:10.1002/2014SW001147.

Matéo-Vélez, J. C., Sicard, A., Payan, D., Ganushkina, N., Meredith, N. P., & Sillanpäa, I. (2018). Spacecraft surface charging induced by severe environments at geosynchronous orbit. Space Weather, 16(1), 89-106.

NASA (2011), "Mitigating in-space charging effects – a guideline," NASA Technical Handbook NASA-HDBK-4002A, March 3, 2011. https://standards.nasa.gov/standard/NASA/NASA-HDBK-4002

O'Brien, T. P. (2009), SEAES-GEO: A spacecraft environmental anomalies expert system for geosynchronous orbit, Space Weather, 7, S09003, doi:10.1029/2009SW000473.

Rodgers, D. J. and K. A. Ryden, Internal charging in space, Proc. 7th Spacecraft Charging Technol. Conf., Noordwijk, The Netherlands, Edited by R. A. Harris, European Space Agency, p. 25, paper ESA SP-476, 2001.

Roeder, J. L. (1994), Specification of the plasma environment at geosynchronous orbit in the energy range 87 eV to 288 keV, Aerospace Report No. TR-94(4940)-6.

Thomsen, M. F., M. G. Henderson, and V. K. Jordanova (2013), Statistical properties of the surface-charging environment at geosynchronous orbit, Space Weather, 11, pp. 237--244, 2013, doi: 10.1002/swe.20049

Wilkinson, D. C. (1994). National Oceanic and Atmospheric Administration's spacecraft anomaly data base and examples of solar activity affecting spacecdraft. Journal of Spacecraft and Rockets, 31, 160-165.